Title

Siderophore Immunization Restricted Colonization of Adherent-Invasive Escherichia coli and Ameliorated Experimental Colitis

Journal

mBio, 13(5)

ISSN

2161-2129

Authors

Gerner, Romana R

Hossain, Suzana

Sargun, Artur

et al.

Publication Date

2022-10-26

DOI

10.1128/mbio.02184-22

AMERICAN SOCIETY FOR MICROBIOLOGY | mBio®

RESEARCH ARTICLE

Siderophore Immunization Restricted Colonization of Adherent-Invasive *Escherichia coli* and Ameliorated Experimental Colitis

Romana R. Gerner,[a] Suzana Hossain,[a] Artur Sargun,[b]* Kareem Siada,[a] Grant J. Norton,[a] Tengfei Zheng,[b] Wilma Neumann,[b]§ Sean-Paul Nuccio,[a] Elizabeth M. Nolan,[b] Manuela Raffatellu[a,c,d]

[a]Department of Pediatrics, Division of Host-Microbe Systems and Therapeutics, University of California San Diego, La Jolla, California, USA
[b]Department of Chemistry, Massachusetts Institute of Technology, Cambridge, Massachusetts, USA
[c]Center for Microbiome Innovation, University of California San Diego, La Jolla, California, USA
[d]Chiba University-University of California-San Diego Center for Mucosal Immunology, Allergy, and Vaccines (CU-UCSD cMAV), La Jolla, California, USA

ABSTRACT Inflammatory bowel diseases (IBD) are characterized by chronic inflammation of the gastrointestinal tract and profound alterations to the gut microbiome. Adherent-invasive *Escherichia coli* (AIEC) is a mucosa-associated pathobiont that colonizes the gut of patients with Crohn's disease, a form of IBD. Because AIEC exacerbates gut inflammation, strategies to reduce the AIEC bloom during colitis are highly desirable. To thrive in the inflamed gut, *Enterobacteriaceae* acquire the essential metal nutrient iron by producing and releasing siderophores. Here, we implemented an immunization-based strategy to target the siderophores enterobactin and its glucosylated derivative salmochelin to reduce the AIEC bloom in the inflamed gut. Using chemical (dextran sulfate sodium) and genetic (*Il10*$^{-/-}$ mice) IBD mouse models, we showed that immunization with enterobactin conjugated to the mucosal adjuvant cholera toxin subunit B potently elicited mucosal and serum antibodies against these siderophores. Siderophore-immunized mice exhibited lower AIEC gut colonization, diminished AIEC association with the gut mucosa, and reduced colitis severity. Moreover, Peyer's patches and the colonic lamina propria harbored enterobactin-specific B cells that could be identified by flow cytometry. The beneficial effect of siderophore immunization was primarily B cell-dependent because immunized *mu*MT$^{-/-}$ mice, which lack mature B lymphocytes, were not protected during AIEC infection. Collectively, our study identified siderophores as a potential therapeutic target to reduce AIEC colonization and its association with the gut mucosa, which ultimately may reduce colitis exacerbation. Moreover, this work provides the foundation for developing monoclonal antibodies against siderophores, which could provide a narrow-spectrum strategy to target the AIEC bloom in Crohn's disease patients.

IMPORTANCE Adherent-invasive *Escherichia coli* (AIEC) is abnormally prevalent in patients with ileal Crohn's disease and exacerbates intestinal inflammation, but treatment strategies that selectively target AIEC are unavailable. Iron is an essential micronutrient for most living organisms, and bacterial pathogens have evolved sophisticated strategies to capture iron from the host environment. AIEC produces siderophores, small, secreted molecules with a high affinity for iron. Here, we showed that immunization to elicit antibodies against siderophores promoted a reduction of the AIEC bloom, interfered with AIEC association with the mucosa, and mitigated colitis in experimental mouse models. We also established a flow cytometry-based approach to visualize and isolate siderophore-specific B cells, a prerequisite for engineering monoclonal antibodies against these molecules. Together, this work could lead to a more selective and antibiotic-sparing strategy to target AIEC in Crohn's disease patients.

KEYWORDS *Escherichia coli*, gut inflammation, immunization, inflammatory bowel disease, iron utilization, mucosal immunity, siderophores

Editor K. Heran Darwin, New York University School of Medicine

Address correspondence to Manuela Raffatellu, manuelar@ucsd.edu.

*Present address: Artur Sargun, A. A. Martinos Center for Biomedical Imaging, Department of Radiology, Massachusetts General Hospital, Harvard Medical School, Charlestown, MA, United States.

§Present address: Wilma Neumann, Inorganic Chemistry I, Ruhr-University Bochum, Bochum, Nordrhein-Westfalen, Germany.

The authors declare a conflict of interest. E.M.N. and M.R. hold a patent related to this work.

This article is a direct contribution from Manuela Raffatellu, a Fellow of the American Academy of Microbiology, who arranged for and secured reviews by Harry Mobley, University of Michigan Medical School, and Janelle Arthur, University of North Carolina at Chapel Hill.

Received 28 July 2022
Accepted 3 August 2022
Published 12 September 2022

Crohn's disease (CD) belongs to the spectrum of inflammatory bowel diseases (IBD) and is characterized by chronic inflammation of the gastrointestinal (GI) tract. The pathophysiology of CD is complex and involves dysregulated immune responses toward environmental and microbial triggers, disruptions of epithelial barrier integrity, and alterations of the gut microbiota composition in genetically susceptible individuals (1–5). The healthy human gut microbiota is dominated by obligate anaerobic microbes belonging to the phyla *Firmicutes* and *Bacteroidetes*, whereas the oxidative environment of the inflamed gut, such as in IBD, typically results in a dramatically reduced abundance of these organisms (6, 7). By contrast, other microbes, particularly select facultative anaerobic members of the *Enterobacteriaceae* family (order *Enterobacterales*), thrive during inflammation (8). In addition to the typical compositional shifts in IBD-associated microbial communities, specific bacterial species with potentially disease-triggering properties are also enriched in IBD patients (9). Nevertheless, the causal relationships between such microbes and IBD pathophysiology remain a matter of debate (10). *Escherichia coli* is a prototypical member of the *Enterobacteriaceae* family and encompasses many different strains, including various commensals and human pathogens (11–13). Adherent-invasive *E. coli* (AIEC) is a functionally distinct and more virulent type of *E. coli* that is frequently recovered from the inflamed ileal and colonic mucosa of CD patients (14–17). Contrary to traditional pathogenic *E. coli*, AIEC strains do not harbor a unique genetic signature and, thus, are typically identified by their pathogenic phenotypes. These characteristics include adherence, attachment, and invasion of intestinal epithelial cells, as well as survival and replication within macrophages, all of which are linked to CD progression (18, 19). AIEC is well adapted to the inflammatory environment of the IBD gut, and some of its phenotypic traits have been linked to virulence-associated genes (20). These traits include genes encoding propanediol utilization, adhesion, cell invasion, and iron acquisition, which are overrepresented in AIEC relative to nonpathogenic *E. coli* strains (15, 21–24).

Even though it is widely accepted that the bloom of AIEC in the inflamed gut is detrimental, there are no treatment options to selectively eradicate AIEC from the gut mucosa of IBD patients, although a few interventions are being tested in ongoing clinical trials (25). Antibiotic treatment in the context of CD remains controversial due to the induction of bacterial dysbiosis and is, thus, restricted to infectious complications or in the postoperative setting (7). In addition, the emerging threat of antimicrobial resistance further complicates the use of antibiotics, and antibiotics have been associated with exacerbation of AIEC infection in IBD patients (26). Vaccines could be major alternatives to antibiotics for AIEC infection. In addition to preventing disease, vaccines generate polyclonal antibody responses and induce cellular immunity, which decrease the risk and emergence of escape mutations (27).

A promising strategy to target *Enterobacteriaceae*, including *E. coli*, is the development of siderophore-based vaccines (28, 29). Siderophores are iron-chelating secondary metabolites that are biosynthesized under conditions of iron limitation (such as colitis), released by producers to scavenge iron from the environment, and then imported by dedicated uptake machinery to provide iron to the cell. As such, siderophore-mediated iron acquisition is one way that certain bacterial species overcome iron limitation and promote their growth and competition with the gut microbiota (30, 31). Accordingly, siderophores constitute important fitness and virulence factors of many Gram-negative pathogens (31–33). IBD-associated AIEC strains harbor several siderophore and ferric iron uptake genes, which are also present in extraintestinal pathogenic *E. coli* (15, 19, 34). Enterobactin (Ent) is an archetypal, catecholate-type siderophore broadly utilized by *Enterobacteriaceae*, including *E. coli*, to acquire iron from the host (35). The biological importance of Ent is exemplified by the coevolution of the host protein lipocalin-2 (Lcn2), which binds to iron-associated Ent (Fe-Ent) and thereby impedes bacterial iron acquisition (36, 37). In addition to Ent, several *Enterobacteriaceae*, including mostly pathogenic *E. coli* strains, produce C-glucosylated Ent, known as salmochelin (GlcEnt), which is not bound by Lcn2 and thereby enables evasion of this host-mediated antimicrobial response (38).

We have previously demonstrated that immunization of mice with Ent conjugated to the mucosal adjuvant cholera toxin subunit B (CTB) elicits a strong mucosal immune

response against microbe-derived Ent and GlcEnt and conferred protection against intestinal infection with *Salmonella enterica* serovar Typhimurium (29). Because Ent and GlcEnt are also key virulence factors for *E. coli* (30, 39), and the genes for their synthesis and transport are expressed by AIEC in the inflamed gut (40), we hypothesized that immunization against Ent/GlcEnt may limit the AIEC bloom during colitis. Here, we showed that Ent immunization reduced AIEC colonization of the inflamed gut, particularly the association of AIEC with the intestinal mucosa, and ameliorated colitis in mice. We also identified Ent-specific B cells in the Peyer's patches and colonic lamina propria of immunized mice, which could be visualized and isolated by a flow cytometry-based approach. These findings set the basis for the development of monoclonal antibodies against siderophores, which could provide a narrow-spectrum strategy to target AIEC in patients with CD.

RESULTS

CTB-Ent immunization reduced AIEC colonization and ameliorated colitis in *Lcn2*$^{-/-}$ mice. During infection, Ent is captured by the host protein Lcn2, which limits Ent-mediated iron acquisition and hinders bacterial growth (37). We previously showed that intranasal immunization of mice with Ent conjugated to the mucosal adjuvant cholera toxin subunit B (CTB), hereafter CTB-Ent, elicited specific antibodies against both Ent and GlcEnt (29). Thus, we sought to investigate the role of CTB-Ent immunization in mice that lack a functional Lcn2. The AIEC strain NRG857c (isolated from a CD patient) harbors several genes involved in siderophore production and iron metabolism, including genes for the synthesis and transport of Ent, GlcEnt, yersiniabactin, and aerobactin, and heme uptake (15). To test whether AIEC NRG857c colonized mice in our facility, *Lcn2*$^{-/-}$ mice were administered a single dose of oral streptomycin 24 h before infection with 10^9 CFU of AIEC NRG857c or mock. Streptomycin depleted the commensal microbiota and thereby facilitated AIEC colonization of the mouse gut (Fig. S1A and B). During AIEC infection, dextran sulfate sodium (DSS) was provided in the drinking water to induce colitis (Fig. S1A to D), thereby driving iron limitation and consequently promoting microbial siderophore secretion. Mice were stably colonized with AIEC throughout the experiments, and AIEC infection in addition to DSS administration further aggravated colonic inflammation than DSS alone (Fig. S1C to D).

Next, we tested whether Ent immunization could mimic the Ent-neutralizing function of Lcn2 in the context of AIEC infection. *Lcn2*$^{-/-}$ mice were immunized with 100 μg CTB-Ent or CTB (mock control) intranasally, followed by a boost after 14 days as described previously (29). After 28 days from the first dose, mice were administered streptomycin 24 h before AIEC infection (14, 16). *Lcn2*$^{-/-}$ mice immunized with either CTB or CTB-Ent during AIEC infection exhibited a similar weight course (Fig. 1A). Analysis of fecal AIEC over time revealed that mice immunized with CTB-Ent exhibited significantly lower AIEC CFU at 72 h and 96 h postinfection (pi) compared to CTB control mice (Fig. 1B). Even though colon lengths were comparable in both groups (colonic shortening is a proxy for intestinal inflammation), mice immunized with CTB-Ent exhibited an overall decreased histological colitis severity (Fig. 1C).

To assess whether CTB-Ent immunization induced specific anti-siderophore antibodies, we evaluated anti-Ent and anti-GlcEnt titers in serum and feces from immunized mice using our in-house ELISA (29), which employed biotinylated Ent or GlcEnt (Fig. S2) bound to streptavidin-coated plates. Both fecal anti-Ent Immunoglobulin (Ig) A and serum anti-Ent Ig were significantly elevated in mice immunized with CTB-Ent after AIEC infection, compared to the CTB control group (Fig. 1D). Fecal and serum anti-GlcEnt titers were also higher in CTB-Ent immunized mice, although this increase was not statistically significant (Fig. 1G).

Biofilm formation and association with the intestinal epithelium is a common pathogenic feature of AIEC (41, 42). To visualize the spatial relationship of AIEC with commensal microbes and the gut epithelium, we performed bacterial fluorescence *in situ* hybridization (FISH) from proximal colon samples obtained at 96 h pi. In CTB-immunized mice, AIEC was either located in close proximity to or attached to the intestinal epithelium and within crypts (Fig. 1F). In stark contrast, AIEC was mostly confined to the intestinal lumen of mice immunized with CTB-Ent without adhering to the epithelial layer (Fig. 1F). Instead, microbes detected with the pan-bacterial *Eubacteria* probe (e.g., the microbiota) were adjacent to the epithelial lining and separated AIEC from the mucosa (Fig. 1F).

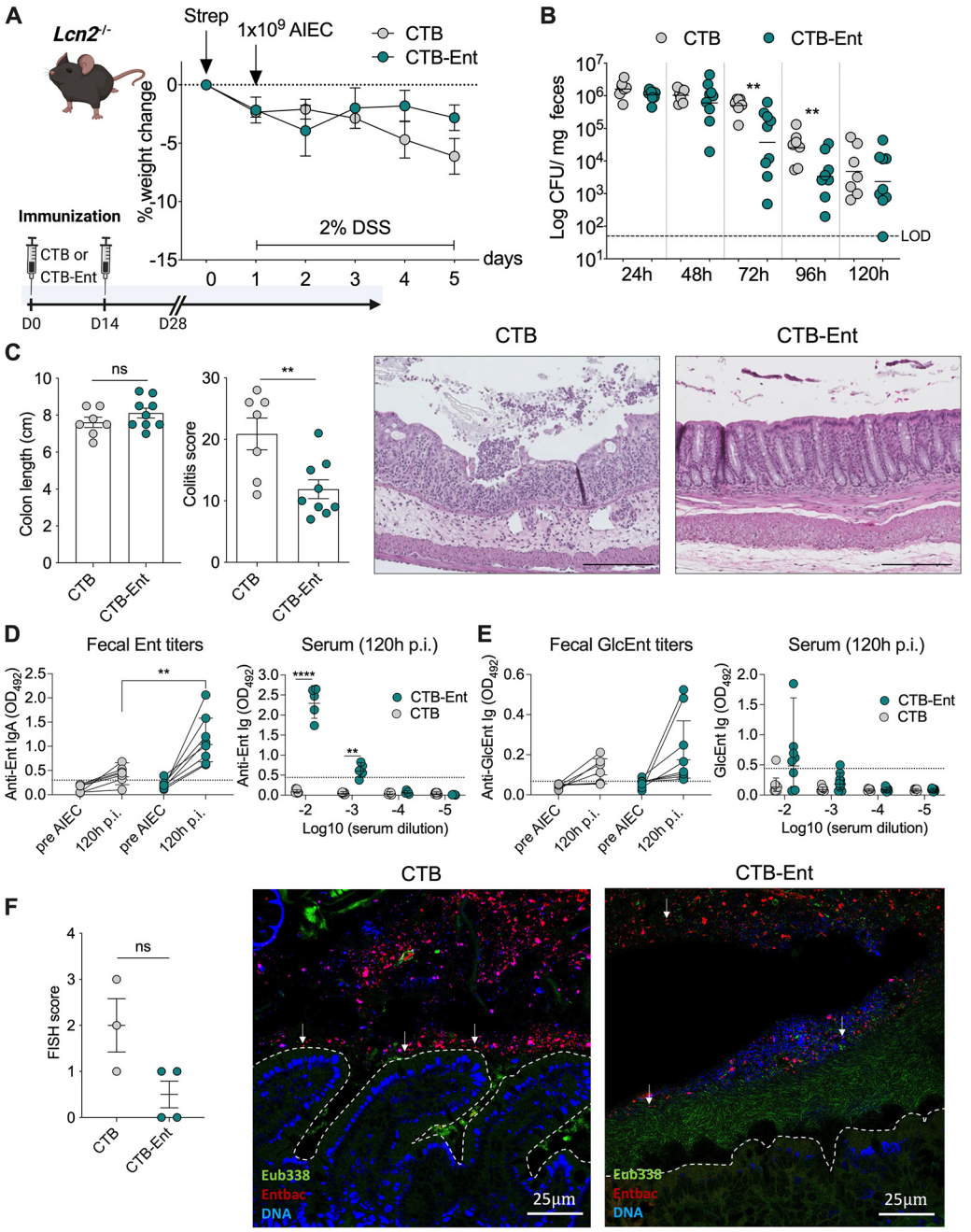

FIG 1 CTB-Ent immunization protected mice from AIEC infection in the absence of Lcn2. (A) Experimental timeline (schematic created with BioRender) and weight loss during AIEC infection in *Lcn2*$^{-/-}$ mice. Mice received 100 μg intranasal CTB or CTB-Ent at day 0, followed by a booster 14 days later. Animals were considered fully immunized 28 days after the initial immunization. (B) Fecal AIEC shedding was monitored in mice immunized with CTB (gray circles) or CTB-Ent (green circles) over time. Each circle represents a mouse. The dashed horizontal line indicates the limit of detection (LOD). (C) Colon lengths and colitis scores were assessed on day 5 post-AIEC infection. Representative pictures from H&E-stained colonic sections are shown. 100× magnification; Scale bars, 200 μm. (D) Optical density 450 nm (OD_{450}) values of fecal anti-Ent IgA and blood anti-Ent Ig (120 h pi, dilutions indicated in the figure) are shown. Fecal OD_{450} values are shown from undiluted samples (pre-AIEC) or 1:5 dilutions (120 h pi). (E) OD_{450} values for anti-GlcEnt Ig in feces (undiluted) and serum (120 h pi, dilutions indicated in the figure). Assay cutoffs are indicated by dashed lines. (F) FISH scores represent epithelial attachment and epithelial invasion of AIEC in proximal colon sections from FISH experiments. Representative confocal images of each group are shown. The colonic epithelium is highlighted by a white dashed line. AIEC are indicated with white arrowheads. 200× magnification; Scale bars, 25 μm. LOD, limit of detection; pi, postinfection. Data represent mean ± SEM (A, C, and F), geometric mean (B), or geometric mean ± SD (D and E); ns, not significant; **, $P \leq 0.01$; ****, $P \leq 0.0001$.

Together, these data demonstrated that CTB-Ent immunization markedly protected *Lcn2*$^{-/-}$ mice from the development of severe colitis by reducing the colonization and association of AIEC with the gut mucosa. The presence of anti-Ent antibodies also suggested that immunization with CTB-Ent may provide a functional rescue of Lcn2 deficiency.

CTB-Ent immunization reduced AIEC colonization and colitis in WT mice. During IBD and other forms of intestinal inflammation, upregulated Lcn2 production prevents the outgrowth of Ent-dependent microbes (2, 43, 44). Before immunization experiments, we confirmed that wild-type (WT) mice remained colonized with AIEC throughout the experiment (120 h; Fig. S3A and B). Similar to *Lcn2*$^{-/-}$ mice, AIEC infection also exacerbated DSS-induced colitis in WT mice (Fig. S3C). To assess the efficacy of CTB-Ent immunization during AIEC infection in the presence of Lcn2, we immunized and infected WT mice that were littermates of *Lcn2*$^{-/-}$ mice. Following AIEC infection and DSS treatment, both groups exhibited a similar weight course (Fig. 2A) and AIEC colonization levels (Fig. 2B). CTB-Ent immunization, however, resulted in reduced colonic shortening and significantly lower histological colitis scores compared to CTB control mice (Fig. 2C). In line with findings in *Lcn2*$^{-/-}$ mice, CTB-Ent immunization elicited significantly higher levels of anti-Ent (Fig. 2D) and anti-GlcEnt (Fig. 2E) antibodies in feces and serum. FISH analysis from the proximal colon of WT mice immunized with CTB (mock) showed that AIEC was frequently found near the mucus layer or associated with the mucosa (Fig. 2F). In contrast, AIEC was confined to the lumen of WT mice immunized with CTB-Ent (Fig. 2F), akin to what we found in *Lcn2*$^{-/-}$ mice immunized with CTB-Ent (Fig. 1F). Furthermore, AIEC was shielded from the mucosa by a wall of rod-shaped bacteria hybridizing with the *Eubacteria* probe in WT mice immunized with CTB-Ent (Fig. 2F). Thus, Ent immunization protected mice from the development of colitis by limiting AIEC growth and association with the colonic mucosa, even when functional Lcn2 was present.

CTB-Ent immunization protected from aggravated disease in *Il10*$^{-/-}$ mice. To investigate whether Ent immunization is beneficial in a genetic model for IBD, we employed the *Il10*$^{-/-}$ mouse model of colitis (45). Mice with a genetic deficiency for the anti-inflammatory cytokine interleukin (IL)-10 can exhibit a spontaneous bloom of *Enterobacteriaceae* (including *E. coli*) with the progression of intestinal inflammation; however, this expansion strongly depends on the resident enteric microbiota and the microbial environment of the vivarium (46). *Il10*$^{-/-}$ mice in our animal facility do not develop spontaneous colitis, and AIEC infection by itself only marginally induced colitis (Fig. S4). Microbial siderophore secretion is triggered primarily by inflammation-induced iron restriction. We, therefore, surmised that a beneficial effect of CTB-Ent immunization would especially be observed during more severe intestinal inflammation. Therefore, we utilized a piroxicam-accelerated *Il10*$^{-/-}$ colitis model as previously described (47). Following immunization, mice received a piroxicam-fortified diet for 10 consecutive days before inoculation with 10^9 AIEC CFU. In this model AIEC colonized mice to high levels without the need for streptomycin pretreatment.

Il10$^{-/-}$ mice that were mock-immunized with CTB developed severe disease and lost approximately 17% body weight by day 5 post-AIEC infection (Fig. 3A). In stark contrast, *Il10*$^{-/-}$ mice immunized with CTB-Ent only lost approximately 4% of their body weight 1 day after AIEC infection, and fully recovered by day 5 (Fig. 3A). *Il10*$^{-/-}$ mice immunized with CTB-Ent also showed fewer fecal AIEC beginning at 48 h pi and continuing until the end of experiments. Some immunized mice completely lost AIEC colonization (6 out of 10; Fig. 3B). Colonic shortening as a proxy for intestinal inflammation and histological colitis scores were markedly reduced in *Il10*$^{-/-}$ mice immunized with CTB-Ent compared to CTB controls (Fig. 3C). The differences in colitis corresponded with markedly reduced colonic expression of genes encoding the proinflammatory molecules IL-6 and Lcn2 in the CTB-Ent group compared to CTB control mice (Fig. 3D). Siderophore immunization elicited significant levels of fecal anti-Ent IgA and increased systemic anti-Ent Ig (Fig. 3E). We did not detect GlcEnt Ig titers in these animals (unpublished data).

In agreement with FISH analyses from the DSS colitis model experiments, AIEC was frequently found near or attaching to the intestinal epithelial layer in CTB-immunized control *Il10*$^{-/-}$ mice. In *Il10*$^{-/-}$ mice immunized with CTB-Ent, AIEC was instead primarily located in the colonic lumen (Fig. 3F).

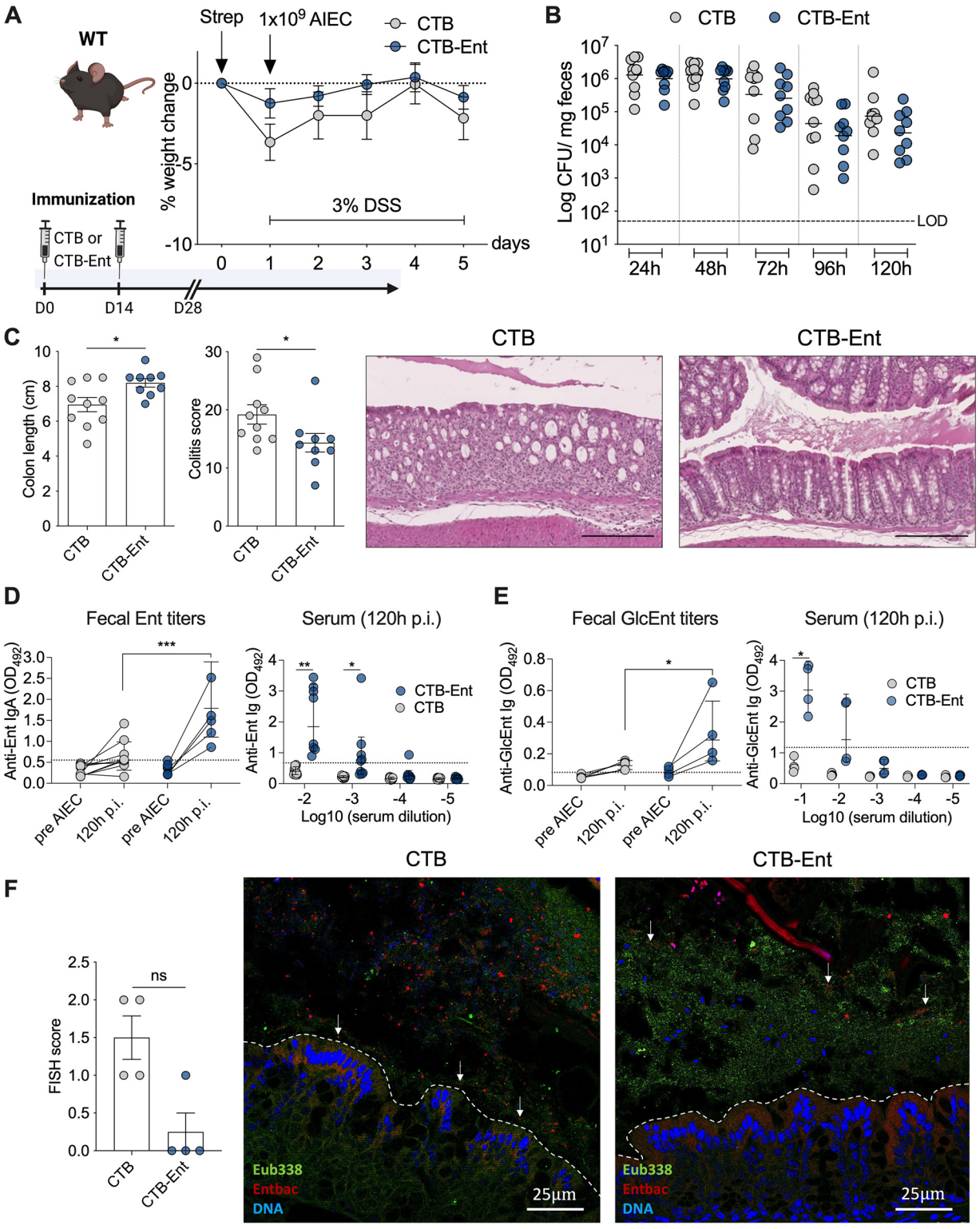

FIG 2 CTB-Ent immunization conferred protection from AIEC-mediated colitis in WT mice (Lcn2 proficient). (A) Experimental timeline (schematic created with BioRender) and weight loss during AIEC infection in WT mice. Mice received 100 μg intranasal CTB or CTB-Ent at day 0 followed by a booster 14 days later. Animals were considered fully immunized 28 days after the initial immunization. (B) Fecal AIEC shedding was monitored in mice immunized with CTB (gray circles) or CTB-Ent (blue circles) over time. Each circle represents a mouse. The dashed horizontal line indicates the limit of detection (LOD). (C) Colon lengths, histopathology colitis scores, and representative H&E-stained colon sections are shown. 100× magnification; Scale bars, 200 μm. (D) Ent-specific IgA levels in feces or Ig in serum are shown as the OD_{450} values. (E) OD_{450} values of fecal and systemic anti-GlcEnt Ig. Fecal anti-Ent OD_{450} values are shown from 1:2 dilutions (at 120 h pi) or undiluted samples (pre-AIEC and GlcEnt). Dashed lines indicate assay cutoffs. (F) Epithelial attachment and epithelial invasion of AIEC in the proximal colon of CTB or CTB-Ent immunized mice were assessed on confocal FISH images and converted into a FISH score. 200× magnification; Scale bars, 25 μm. WT, wild-type; LOD, limit of detection; pi, postinfection. Data represent mean ± SEM (A, C, and F), geometric mean (B), or geometric mean ± SD (D and E); ns, not significant; *, $P \leq 0.05$; **, $P \leq 0.01$; ***, $P \leq 0.001$.

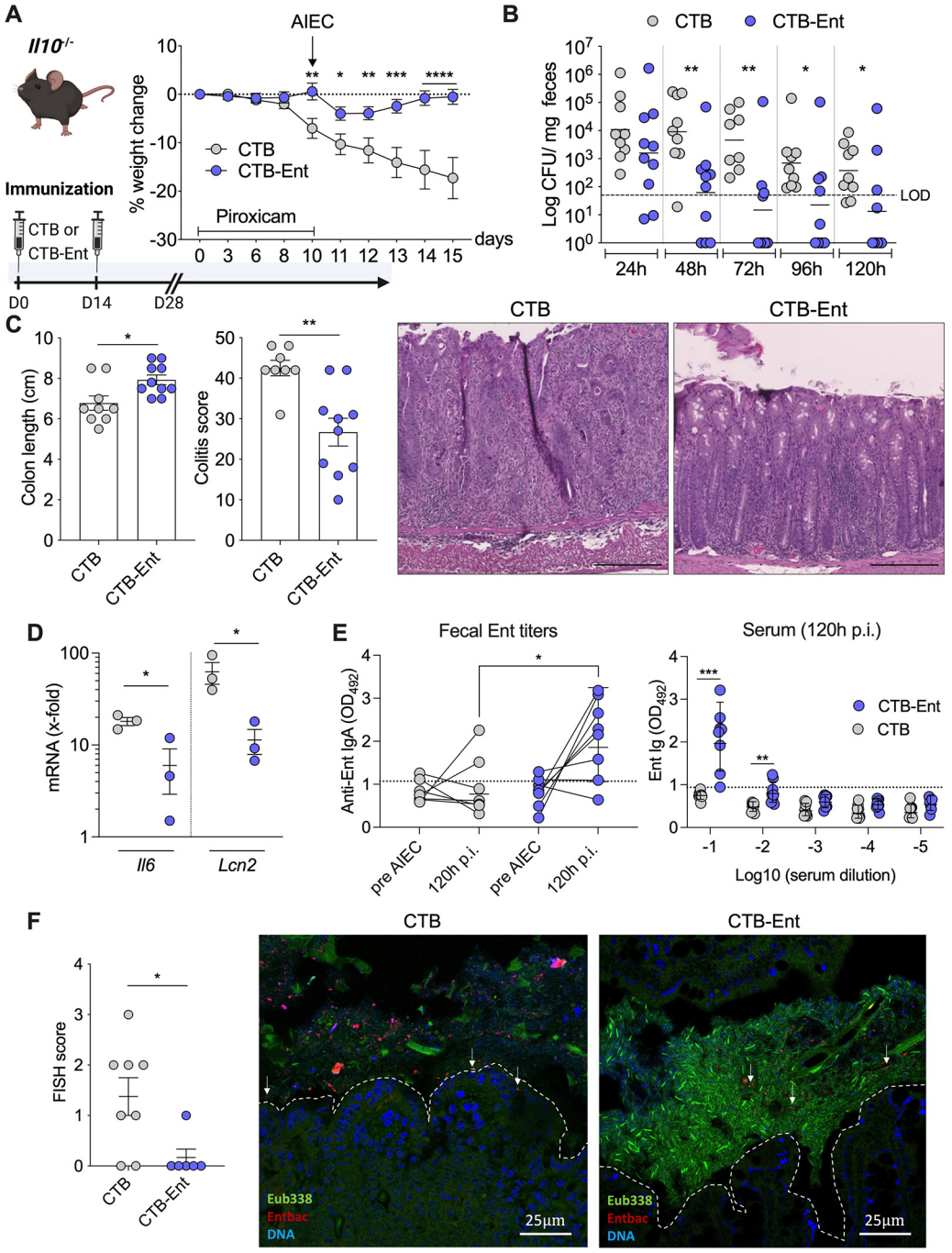

FIG 3 CTB-Ent immunization protected *Il10*$^{-/-}$ mice from severe colitis and reduced the AIEC bloom. (A) Experimental timeline (schematic created with BioRender) along with weight loss in piroxicam-treated *Il10*$^{-/-}$ mice during AIEC infection. Mice were previously immunized with 100 μg intranasal CTB (gray circles) or CTB-Ent (blue circles) at day 0, followed by a booster 14 days later, and were considered fully immunized after 28 days. (B) AIEC in fecal samples throughout the infection. Each circle represents a mouse. (C) Colon lengths and histological colitis scores were assessed at the end of the experiments. Representative pictures from H&E-stained colonic sections are shown. 100× magnification; Scale bars, 200 μm. (D) Colonic mRNA expression of indicated genes was determined in mice immunized with CTB or CTB-Ent 120 h pi. Data are expressed as fold change in comparison to uninfected mice. (E) OD_{450} values of fecal (undiluted) and systemic (dilutions are indicated in the figure) anti-Ent levels are shown. Assay cutoffs are indicated by dashed lines. (F) FISH scores represent the degree of epithelial attachment and invasion. Representative FISH images of the proximal colon of mice are shown. The epithelium is highlighted by a white dashed line. AIEC are indicated with white arrowheads. 200× magnification; Scale bars, 25 μm. LOD, limit of detection; pi, postinfection. Data represent mean ± SEM (A, C, D, and F), geometric mean (B) or geometric mean ± SD (E); ns, not significant; *, $P \leq 0.05$; **, $P \leq 0.01$; ***, $P \leq 0.001$; ****, $P \leq 0.0001$.

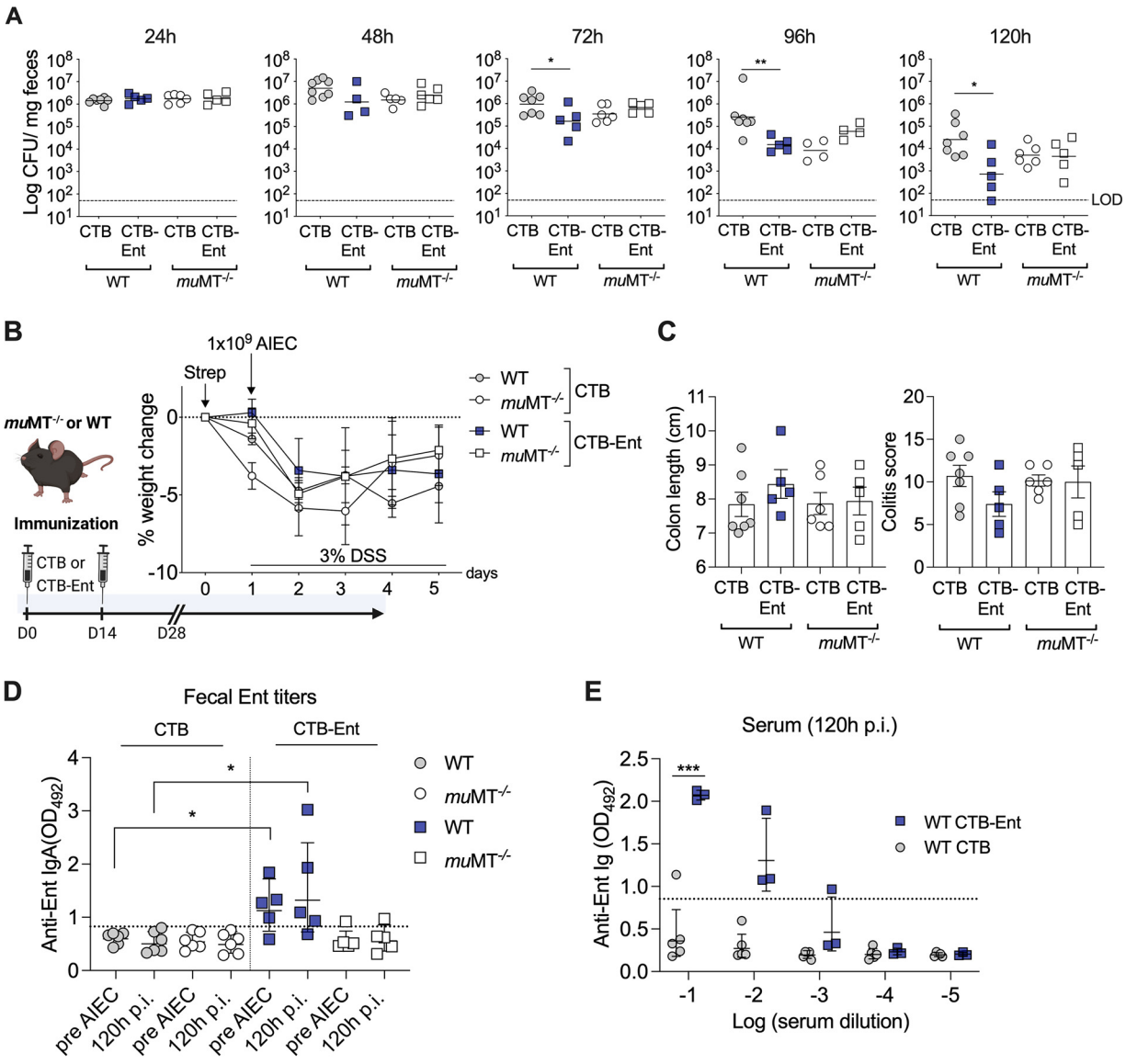

FIG 4 Protection from AIEC infection in mice immunized with CTB-Ent was dependent on B cells. (A) Fecal AIEC of wild-type (WT) and *mu*MT$^{-/-}$ littermate mice that were either immunized with CTB or CTB-Ent before AIEC infection according to the timeline shown in (B). Each symbol represents an individual mouse. (B) Experimental timeline (schematic created with BioRender) along with weight loss during AIEC infection. (C) Colon lengths and histological colitis scores were determined at the end of the experiments. (D) Fecal anti-Ent titers and (E) serum anti-Ent levels of respective groups are shown. Dashed lines indicate the assay cutoffs. WT, wild-type; LOD, limit of detection; pi, postinfection. Data represent geometric mean (A), mean ± SEM (B and C), or geometric mean ± SD (D and E); ns, not significant; *, $P \leq 0.05$; **, $P \leq 0.01$; ***, $P \leq 0.001$.

These data indicated that CTB-Ent immunization strongly protected mice from AIEC-induced severe disease and weight loss, reduced AIEC association with the gut mucosa, and ameliorated colonic inflammation in a genetic model for IBD.

CTB-Ent immunization protected from AIEC infection in a B cell-dependent manner. As CTB-Ent immunization elicited specific anti-siderophore titers and protected mice from AIEC-induced inflammation, we directly tested whether B cell-conferred humoral immunity was responsible for such a phenotype. We immunized B cell-deficient *mu*MT$^{-/-}$ mice and their WT littermates with CTB or CTB-Ent, followed by DSS administration and AIEC infection. On day 3 to 5 post-AIEC infection, CTB-Ent-immunized WT mice exhibited significantly lower fecal AIEC compared to CTB-immunized WT control animals (Fig. 4A). In contrast, no differences in the levels of AIEC colonization (Fig. 4A) and weight loss (Fig. 4B) were observed between *mu*MT$^{-/-}$ mice immunized with either CTB or CTB-Ent. Although there was a trend of longer colons and lower colitis scores in CTB-Ent-immunized WT animals, this difference

did not reach statistical significance (Fig. 4C). WT mice immunized with CTB-Ent displayed specific anti-Ent antibodies in serum and feces (Fig. 4D and E), which were not detected in CTB-immunized WT mice (Fig. 4D and E) or *mu*MT$^{-/-}$ littermates (Fig. 4E, serum data unpublished). Altogether, these data indicated that CTB-Ent immunization triggered B cells to produce anti-Ent antibodies, which resulted in a significant reduction of the fecal AIEC burden in mice.

Siderophore-specific B cells were identified by a flow cytometry-based approach. We next aimed to identify and visualize siderophore-specific B cells produced by mice immunized with CTB-Ent. We previously used ELISPOT assays to identify B cells that secreted anti-siderophore antibodies in Peyer's patches (PP) of mice immunized with CTB-Ent (29). In the gut, PP are key lymphoid structure for the active induction of intestinal immune responses, whereas the lamina propria is the effector site to which activated adaptive immune cells migrate (48, 49). We thus immunized WT mice with CTB-Ent, infected them with AIEC, and collected PP and colons on day 4 pi (Fig. 5A). Single-cell suspensions from PP or colon lamina propria were each pooled from 4 mice and processed for flow cytometry analysis. To identify siderophore-specific B cells, we incubated cells with biotinylated Ent, which we expected to be recognized by the specific surface Ig. Cells were then incubated with two fluorophore-streptavidin conjugates (streptavidin-PE and streptavidin-APC) before staining with surface antibodies (Fig. 5B). Target CD19$^+$/B220$^+$ B cells were identified from live CD45$^+$ cells after exclusion of IgM$^+$ B cells (gating strategy outlined in Fig. 5C). In the final gating step, only B cells with a double-positive signal for streptavidin (i.e., both PE and APC) were included to increase specificity. This approach identified Ent-specific B cells in PP (~1.1% of the parent IgM- population) and the colon lamina propria (~6.6% of the parent IgM- population) of immunized mice (Fig. 5D). To our knowledge, this is the first study to identify siderophore-specific B cells in mammals. Moreover, detection of B cells bound to biotinylated siderophores by utilizing fluorescently labeled streptavidin provides a useful approach for fluorescence-activated cell sorting of siderophore-specific B cells in the future.

DISCUSSION

AIEC is highly prevalent in the gut mucosa of patients with CD, where it is thought to trigger intestinal inflammation (19). Although the first description of AIEC in IBD dates back over 2 decades (50), therapeutic strategies to target AIEC in CD patients are still an unmet medical need. Here, we proposed an immunization strategy to develop antibodies against AIEC siderophores to impede AIEC iron acquisition and thereby hinder AIEC colonization during colitis.

Siderophore immunization elicited mucosal IgA against Ent and GlcEnt. For the first time, we also detected anti-Ent and anti-GlcEnt Ig in the serum, which could play a protective role during systemic infection. Anti-Ent/GlcEnt IgA was produced by B cells localized in small intestinal Peyer's patches as well as in the colonic lamina propria. The production of anti-siderophore antibodies resulted in decreased fecal AIEC shedding and protected mice from severe intestinal inflammation. Protection was most pronounced in *Il10*$^{-/-}$ mice, which otherwise exhibited profound weight loss and aggravated colitis following piroxicam administration and AIEC infection. The impact of siderophore neutralization might thus be greatest in the context of genetic predisposition and severe intestinal inflammation, which is accompanied by the stringent iron limitation that, in turn, would trigger AIEC to produce more siderophores. Although to a lesser extent than in *Il10*$^{-/-}$ mice, we also observed reduced colitis severity in *Lcn2*$^{-/-}$ and WT mice that were immunized with CTB-Ent, despite similar weight courses, and only a transient decrease of fecal AIEC levels compared to respective control-immunized mice.

The beneficial effect(s) of CTB-Ent immunization on various parameters across experiments could be due to a few reasons, including Ig-mediated blockade of secreted Ent and/or GlcEnt, which, in turn, could explain the reduction of AIEC association with the gut mucosa that we observed by FISH and the consequent reduction of gut inflammation, and Ig-mediated neutralization of the proinflammatory responses induced by secreted Ent and/or GlcEnt.

In the healthy gut, the colonic mucus layer consists of mucins, antimicrobial peptides, and secretory IgA (sIgA), which establish an antimicrobial gradient toward the lumen that deters microbes and toxins from the mucosal surface (51–54). During intestinal

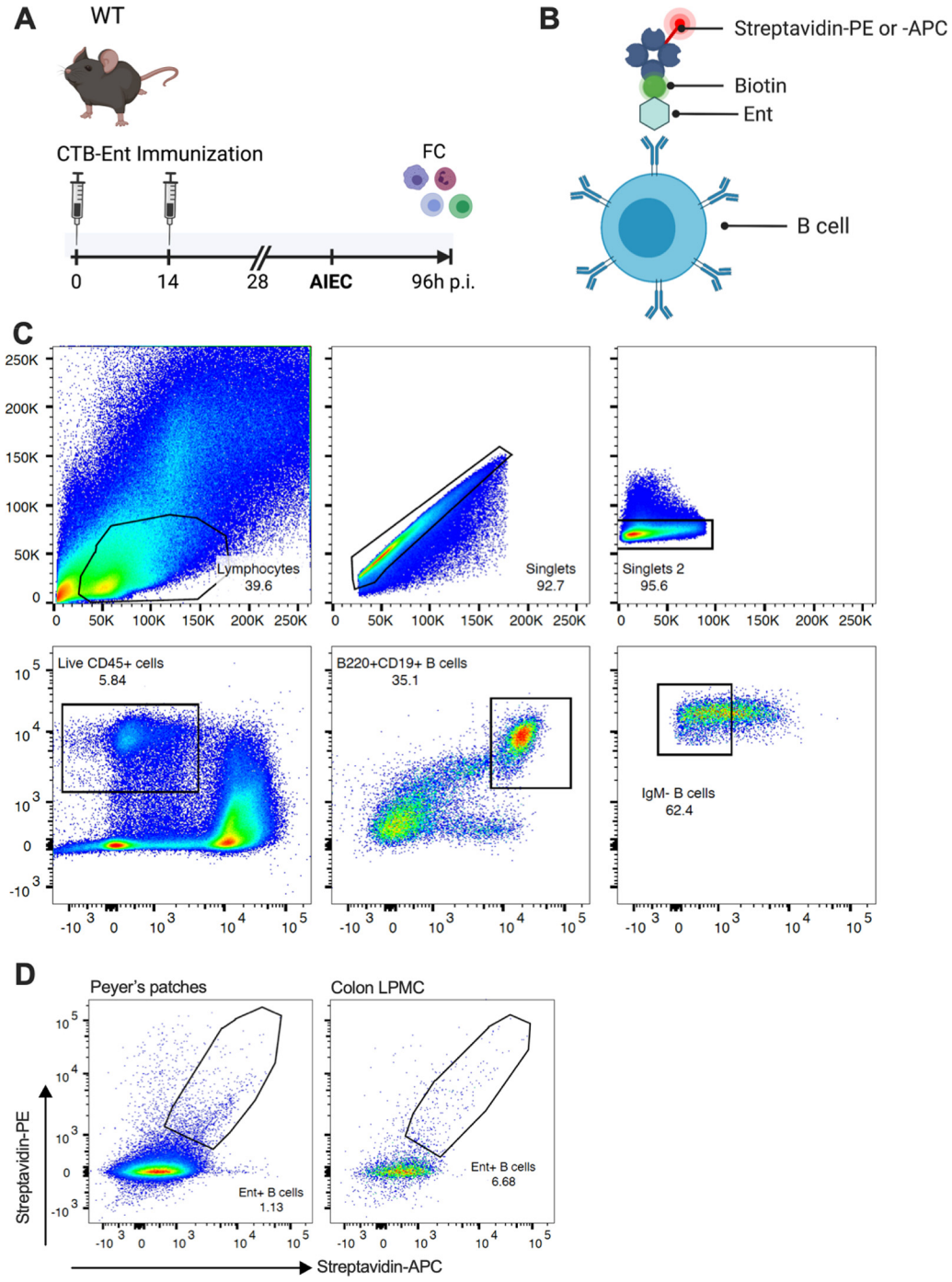

FIG 5 Ent-specific B cells were identified by flow cytometry. (A) WT mice were immunized and infected with AIEC as shown in the schematic (created with BioRender). At 96 h pi, colon lamina propria mononuclear cells (LPMC) and Peyer's patches (PP) were prepared for flow cytometry (FC) staining. (B) Schematic showing how Ent-specific B cells that recognize biotinylated Ent are detected by incubation with both PE- and APC-conjugated streptavidin to increase sensitivity. Created with BioRender. (C) Flow cytometry gating strategy of cells isolated from PP is shown. After identifying the lymphocyte population and excluding doublets, cells were gated on live CD45$^+$ cells followed by identification of CD19$^+$/B220$^+$ double-positive B cells. After exclusion of IgM$^+$ B cells, target B cells (preincubated with Ent-biotin) were identified by PE$^+$-Streptavidin/APC$^+$-Streptavidin double positivity. (D) Representative plots show Ent-specific B cells in PP and colon LPMC from 4 pooled mice, respectively. LPMC, lamina propria mononuclear cells; PP, Peyer's patches; FC, flow cytometry; pi, postinfection.

inflammation or infection with enteric pathogens, proinflammatory mucosal responses further limit microbial access to the epithelium (55). However, certain pathogens, including AIEC, frequently exploit inflammation and thrive (19, 56). In our CTB-immunized mice, independent of the genotypes (*Lcn2*$^{-/-}$, WT, and *Il10*$^{-/-}$ mice), AIEC was not only found in the

gut lumen (reflected by the fecal CFU), but also in close contact with the gut mucosa. In contrast, in mice immunized with CTB-Ent, AIEC was mostly confined to the intestinal lumen and did not come in close contact with the gut mucosa (Fig. 1F, 2F, and 3F). Several studies have demonstrated that the fecal microbiota can differ substantially from mucosa-associated bacterial communities (7, 57–60). In IBD, AIEC and other mucosa-associated microbes have been implicated as important drivers of intestinal inflammation compared to luminal microbes (7). In this context, iron acquisition via siderophores might be particularly critical for sustaining colonization adjacent to the epithelial surface, where the mucus is highly viscous and where iron-restricting antimicrobial proteins, such as Lcn2 and lactoferrin, as well as sIgA concentrations, are highest (51, 53, 54, 61). Thus, Ig-mediated siderophore neutralization may limit the ability of AIEC to closely attach to and/or invade the mucosal surface, resulting in decreased colonic inflammation. Future studies are warranted to further elucidate the exact role of Ent and GlcEnt in such a context.

A second reason that could explain the reduced colitis in mice immunized with CTB-Ent may be due to blockade of proinflammatory responses induced by secreted Ent and/or GlcEnt. Anti-siderophore sIgA likely captures siderophores, rendering them inaccessible to microbes, and neutralizes their proinflammatory properties. This idea is supported by studies undertaken in lung and gut epithelial cells, which demonstrated that iron-free Ent acts as a danger signal, eliciting epithelial IL-8 secretion that is amplified by Lcn2 (62, 63).

Siderophores and their cognate receptors are among the virulence factors employed by AIEC to overcome host barriers and efficiently colonize the gut (15, 19, 40). A recent study utilized an elegant *in vivo* genetic screen and demonstrated that iron acquisition systems were upregulated during AIEC colonization (40). Besides Ent/GlcEnt, other siderophores that evade Lcn2-mediated immunity like aerobactin and yersiniabactin are of critical importance for AIEC virulence (15, 40, 64). For example, yersiniabactin has been shown to promote intestinal fibrosis in *Il10*$^{-/-}$ mice in the absence of binding to its cognate receptor (64).

In our study, anti-siderophore antibodies conferred protection from AIEC colonization and exacerbation of colitis in both *Lcn2*$^{-/-}$ and WT (i.e., Lcn2-proficient) mice. These results might be explained by (i) functional rescue of Lcn2 deficiency by anti-Ent antibodies in *Lcn2*$^{-/-}$ mice, and (ii) antibody-dependent neutralization of GlcEnt (which evades Lcn2) in WT animals. *Il10*$^{-/-}$ mice, however, were strongly protected from AIEC-induced exacerbated colitis even though we only detected anti-Ent antibodies (despite lower titers compared to *Lcn2*$^{-/-}$ and WT mice), but no measurable anti-GlcEnt antibodies. The reduced antibody titers in *Il10*$^{-/-}$ mice might be a consequence of extended administration of piroxicam, a nonsteroidal anti-inflammatory drug (NSAID) that was necessary to induce colitis in our *Il10*$^{-/-}$ colony. NSAIDs have been associated with blunted immune responses, particularly when administered prophylactically (65). Moreover, IL-10 itself is a critical proliferation and differentiation factor for B cells (66), which could also contribute to explaining the decreased antibody titers. Of note, *Il10*$^{-/-}$ mice secrete high levels of mucosal Lcn2 to prevent the outgrowth of Ent-dependent microbes during intestinal inflammation (43). Together, in *Il10*$^{-/-}$ mice, anti-Ent antibodies and Lcn2 could act synergistically to curb AIEC infection and reduce intestinal inflammation. It is also possible that Ent might be essential for certain steps during AIEC infection, despite the presence of Lcn2, and independently of siderophores like yersiniabactin and salmochelin. Thus, the siderophore repertoire of specific AIEC strains might provide context-specific advantages during colitis and dictate the impact of AIEC on host physiology and pathology. Future studies are needed to investigate the relative contribution of other iron uptake systems to AIEC pathogenesis, and whether CTB-Ent immunization conferred greater protection if mice are infected with AIEC strains engineered to only uptake Ent/GlcEnt, but not other siderophores.

Siderophore utilization is not restricted to microbial pathogens. A variety of gut microbes, including nonpathogenic commensals, such as *E. coli* and *Bacteroides thetaiotaomicron*, as well as oral *Rothia* spp., employ Ent for iron acquisition (37, 67, 68). We expect that the anti-Ent antibodies generated by our immunization approach are not specific to pathogen-derived siderophores. Thus, it will be essential to investigate the impact of Ent

immunization on the gut microbiota composition in the absence of infection or inflammation. In a previous study, we found that immunization of mice with CTB-Ent did not affect the gut microbiota before infection but was associated with an expansion of *Lactobacillus* spp. and a reduction of *Proteobacteria* during *Salmonella* infection (29). Nevertheless, short-term blockade of siderophores with oral administration of neutralizing antibodies would likely have minimal impact on the commensal microbiota, contrary to the extensive damage of antibiotics on gut bacteria (69).

In conclusion, our work established a proof of concept for siderophores as a valuable target to reduce AIEC-exacerbated colitis and sets the basis for future studies to engineering monoclonal antibodies to target these molecules.

MATERIALS AND METHODS

Bacterial strains. The AIEC strain NRG857c (O83:H1) (14) was obtained from Alfredo Torres (UTMB Health) and Brian Coombes (McMaster University, ON, Canada). For animal infections, AIEC was cultured overnight in Miller Luria broth (LB; 10 g/L NaCl) media containing chloramphenicol (Cm; 0.03 mg/mL) at 37°C with shaking. The following day, bacteria from overnight cultures were washed, diluted, and resuspended in PBS, to a concentration of 5×10^9 CFU/mL.

Siderophore conjugates. CTB-Ent and Biotin-Ent were synthesized as previously described (29). Multiple batches of CTB-Ent were prepared and utilized throughout these immunization studies. Biotin-DGE (DGE, diglucosylated enterobactin, also known as GlcEnt or salmochelin) was prepared chemoenzymatically using the C-glucosyltransferase IroB (Fig. S2) (38, 70). A 15-mL solution containing 100 mM Ent-Biotin, 600 mM uridine diphosphoglucose (UDP-glucose, Sigma), 5 mM $MgCl_2$, and 1 mM IroB was prepared in 75 mM Tris-HCl buffer at pH 8.0 and divided into 15 ~1000 μL aliquots. These reaction aliquots were incubated at room temperature for 3.5 h and then quenched with the addition of 200 μL 3% trifluoroacetic acid (TFA) (aq). The quenched reaction aliquots were combined in a 50-mL polypropylene falcon tube and lyophilized to dryness. The resulting solid was dissolved in 3 mL of 1:1 MeCN/H_2O and the resulting mixture was centrifuged (13,000 rpm, 10 min). Biotin-DGE was purified from the supernatant by semipreparative HPLC using an Agilent 1200 series high-performance liquid chromatography (HPLC) instrument outfitted with an Agilent Zorbax reverse-phase C18 column (5 μm, 9.4 × 250 mm) at a flow rate of 4 mL/min and a solvent gradient of 10 to 45% B over 7.5 min (solvent A, filtered Milli-Q water with 0.1% TFA; solvent B, HPLC grade MeCN from EMD Millipore with 0.1% TFA; the method began with a 5 min equilibration at 10% B). The purity and identity of Biotin-DGE were determined by analytical HPLC and high-resolution mass spectrometry (Fig. S2A). [M+H]+ m/z cald. 1519.4941, found 1519.4965.

Animal immunization and infection. All animal experiments were approved by the Institutional Animal Care and Use Committee at the University of California, San Diego (protocol number S17107). Specific pathogen-free *Lcn2*$^{-/-}$ mice, *mu*MT$^{-/-}$ mice, their respective wild-type littermates, and *Il10*$^{-/-}$ mice were housed and bred at UCSD. Six- to eight-week-old female and male mice were immunized by intranasal administration of 100 μg of either CTB (Sigma) or CTB-Ent (in PBS), followed by a boost with 100 μg of the same compound 14 days after initial immunization as previously described by our group (29). Before and during infection, mice were regularly monitored for endogenous *E. coli* by plating fecal homogenates on selective MacConkey agar and CFU compared to numbers derived from Cm plates. No Cm-resistant microbes other than AIEC were detected in our animals. One to 4 weeks after complete immunization, *Lcn2*$^{-/-}$ mice, *mu*MT$^{-/-}$ mice, and their respective wild-type littermates, were administered streptomycin (1 mg/g body weight in PBS) by oral gavage followed by infection with 10^9 CFU AIEC 24 h later. To induce colitis, 2 to 3% DSS (MP Biomedicals) was provided in the drinking water throughout the infection. *Il10*$^{-/-}$ mice received a piroxicam-substituted diet (100 ppm; Teklad custom research diets, Envigo) for 10 days before infection with 10^9 CFU AIEC. Weight, fecal AIEC shedding, and anti-Ent/GlcEnt mucosal antibody responses were monitored throughout the experiment. On day 5 pi, mice were euthanized by CO_2 asphyxiation and gut tissues and blood were collected for further analysis.

AIEC enumeration and preparation of fecal supernatants for ELISA. Fresh fecal samples were collected before and after immunization, and daily during AIEC infection. Fecal samples were weighed, resuspended in 1 mL of PBS, and homogenized on a vortex shaker. AIEC was enumerated by plating serial dilutions on LB agar plates containing Cm and incubated at 37°C overnight. For antibody titer quantification, fecal homogenates were centrifuged at 10,000 × *g* for 10 min and the supernatants were collected and stored at −20°C until further analyses.

Histopathological evaluation. For histological colitis assessment, mid to distal colon samples were fixed in 10% buffered formalin and processed according to standard procedures for paraffin embedding. The 5 μm sections were stained with hematoxylin and eosin (H&E) and slides were scanned on a NanoZoomer slide scanner and visualized using NDP.view2 viewer software (both Hamamatsu). Colonic inflammation was scored in a blinded fashion using a semiquantitative scoring system as described previously (maximum score = 48) (43).

Bacterial fluorescence *in situ* hybridization. Proximal colonic tissue samples were harvested and fixed in Carnoy's fixative for a minimum of 72 h and then processed as previously described (54). Tissue sections (5 μm) were deparaffinized followed by hybridization for 4 h at 46°C in the presence of 20% formamide utilizing the following probes as reported earlier (71): pan-bacterial EUB338 (5′-GCTGCCTCCCGTAGGAGT-3′), non-EUB (5′-ACATCCTACGGGAGGC-3′) and species-specific ENTBAC (5′-CCTTGCGGTTGGCTTCAGAT-3′). Probes were labeled at the 5′ and 3′ ends with fluorescein isothiocyanate (FITC), Cy5, or Cy3 (BioTez, Berlin, Germany).

After washing, cell nuclei were stained with Sytox Deep Red Nucleic Acid Stain (Invitrogen) and cover-slipped using ProLong Gold Antifade Reagent (Life Technologies). Samples were viewed and imaged in a blinded fashion on a Leica DMI4000 B inverted confocal microscope. FISH scores were obtained according to a previously reported scoring system with slight modifications (64). Briefly, epithelial attachment and epithelial invasion of microbes hybridizing with the Cy3-ENTBAC probe were assessed in 3 different regions of the proximal colon sample for each mouse. Bacterial quantities were enumerated as described in (64) and converted to a score from 1 to 4 for both parameters (i.e., a maximum score of 8).

RNA isolation and qPCR. Cecal and colonic tissue was snap-frozen in liquid nitrogen and stored at −80°C until further processing. Samples were homogenized with mortar and pestle, and total RNA was extracted utilizing a Qiagen RNeasy Minikit according to the manufacturer's instructions. Reverse transcription was performed with SuperScript IV VILO Master Mix, and gene expression was analyzed with real-time qPCR by utilizing PowerUp SYBR Green Master Mix and a QuantStudio 5 (all Thermo Fisher). Data were analyzed according to the comparative $2-\Delta\Delta Ct$ method, and target gene expression was normalized to *Actb* mRNA (β-actin). Primer sequences were used as follows: *Actb* 5′-GGCTGTATTCCCCTCCATCG-3′ and 5′-CCAGTTGGTAACAATGCCATGT-3′; *Il6* 5′-GAGGATACCACTCCCAACAGACC-3′ and 5′-AAGTGCATCATCGTTGTTCATACA-3′; *Lcn2* 5′-ACATTTGTTCCAAGCTCCAGGGC-3′ and 5′-CATGGCGAACTGGTTGTAGTCCG-3′.

Antibody titer quantification by ELISA. Antibody titers in fecal supernatants and sera were determined by our in-house ELISA as described earlier (29) with minor modifications. Briefly, Streptavidin High Binding Capacity Coated 96-Well Plates (Pierce, Thermo Fisher Scientific) were washed and coated with either biotinylated enterobactin (Biotin-Ent, 1 μg/mL) or salmochelin (Biotin-DGE, 1 μg/m) for 2 h at room temperature (RT). The plates were then washed 3 times with wash buffer (Tris-buffered saline, 0.1% bovine serum albumin [BSA], 0.05% Tween 20), followed by incubation with 100 μL of diluted fecal supernatants or serially diluted sera for 1 h at RT. Subsequently, the plates were washed 3 times and incubated with IgA-HRP or Ig-HRP antibody (both from Southern Biotech; 1:1,000 dilution in wash buffer). Next, 100 μL of the antibody dilution was added to each well, and the plates were incubated for 30 min at RT with gentle rocking. After incubation, the plates were washed 3 times followed by the addition of 100 μL substrate solution (SIGMA*FAST* OPD, Sigma) and incubation for 20 min in the dark. The reaction was quenched by adding 50 μL of 2N hydrogen sulfate (H_2SO_4) to each well. Absorbance was read at an optical density (OD) at 492 nm using a Biotek Epoch Microplate Spectrophotometer. The cutoffs for enzyme-linked immunosorbent assays (ELISAs) were determined for each assay according to a previously described method (72).

LPMC and PP isolation. Lamina propria mononuclear cells were isolated as previously described with minor modifications (43). Briefly, colons were harvested at 96 h pi, flushed with cold PBS (Gibco), and cut longitudinally. Tissue was minced with a scalpel and shaken in calcium/magnesium-free Hank's balanced salt solution (HBSS)/10% fetal bovine serum (FBS) (Life Technologies) containing 1 mM DTT and 2 mM EDTA (Sigma-Aldrich) for 20 min at RT. Subsequently, fragments were vortexed for 4 min at full speed, supernatants removed, and tissue fragments resuspended in HBSS/FBS, followed by another vortex step for 2 min. After removal of supernatant (containing epithelial cells), tissue fragments were transferred into IMDM medium (Life Technologies) supplemented with 20% FBS, 128 U/mL type IV collagenase, and 10 U/mL DNase II (both Sigma-Aldrich), and then rotated at 37°C for 60 min. After digestion, samples were resuspended thoroughly. Suspensions were consecutively filtered through 100/70/40 μm cell strainers and spun down at 350 $\times$ *g* for 10 min.

For PP isolation, structures were visually identified on the antimesenteric side of the small intestine, dissected with curved scissors, and placed into cold PBS/0.5% BSA (flow buffer, FB). To generate single cell suspensions, PP was then ground into the mesh of a 70 μm nylon mesh cell strainer (Thermo Fisher) using the plunger from a 1 mL syringe (BD Biosciences). The cell strainer was flushed with FB and cell suspensions were centrifuged at 350 $\times$ *g* for 10 min, followed by resuspension in FB and further processing for flow cytometry staining.

Flow cytometry. All steps were carried out at 4°C in the dark. Single-cell suspensions from PP and lamina propria were blocked for nonspecific binding followed by a viability staining with Zombie yellow (both BioLegend). After washing with FB at 350 $\times$ *g* for 10 min, cells were incubated with Ent-Bio for 30 min and washed 3 times with FB. Cells were then incubated with the secondary reagents Streptavidin-PE and Streptavidin-APC for 30 min followed by 3 washes with FB. Surface staining was performed using the following monoclonal antibodies: APC/Cy7 anti-mouse CD45 (clone 30F-11), FITC anti-mouse CD19 (clone 6D5), PerCP/Cy5.5 anti-mouse B220 (clone RA3-6B2), and bv421 anti-mouse IgM (clone RMM-1; all from BioLegend) was done for 30 min, followed by 3 washes with FB. Subsequently, antigen-specific B cells were identified by flow cytometry using a BD LSRFortessa (BD Biosciences), based on a PE^{hi}/APC^{hi} double-positive signal. Data were analyzed using FlowJo v10 software.

Statistical analysis. Statistical analysis was performed with GraphPad Prism v9. CFU data were log-normalized before statistical testing. Normality distribution was tested with the Shapiro-Wilk test. For comparison between 2 normally distributed groups, *P* values were calculated by unpaired Student's *t* test. Mann-Whitney *U* was performed for unpaired data sets that are not normally distributed. One-way analysis of variance (ANOVA) with Tukey's multiple-comparison test was used when analyzing more than 2 groups.

SUPPLEMENTAL MATERIAL

Supplemental material is available online only.

FIG S1, TIFF file, 1.9 MB.

FIG S2, TIFF file, 0.3 MB.

FIG S3, TIFF file, 1.3 MB.

FIG S4, TIFF file, 1.2 MB.

ACKNOWLEDGMENTS

This work was mainly supported by the NIH (R01 AI114625 to M.R. and E.M.N.). M.R. and E.M.N. are also supported by R21 AI154644. Work in the M.R. lab is also supported by the NIH grants AI126277 and AI145325, by the Chiba University-University of California-San Diego (UCSD) Center for Mucosal Immunology, Allergy, and Vaccines, and by the UCSD Department of Pediatrics. M.R. also holds an Investigator in the Pathogenesis of Infectious Disease Award from the Burroughs Wellcome Fund. R.R.G. was partly supported by a fellowship from the Max Kade Foundation and by a fellowship from the Crohn's & Colitis Foundation, award number 649744, project title: Siderophore immunization as a selective strategy to target adherent-invasive *E. coli*. Flow cytometry experiments were performed at the Sanford Burnham Prebys Flow Cytometry Core. Histological slides were scanned at the UCSD School of Medicine Microscopy Core Facility, which is supported by the grant P30 NS047101. G.J.N. was partly supported by the NIH training grant T32 DK007202.

E.M.N. and M.R. hold a patent related to this work.

REFERENCES

1. Jostins L, Ripke S, Weersma RK, Duerr RH, McGovern DP, Hui KY, Lee JC, Schumm LP, Sharma Y, Anderson CA, Essers J, Mitrovic M, Ning K, Cleynen I, Theatre E, Spain SL, Raychaudhuri S, Goyette P, Wei Z, Abraham C, Achkar J-P, Ahmad T, Amininejad L, Ananthakrishnan AN, Andersen V, Andrews JM, Baidoo L, Balschun T, Bampton PA, Bitton A, Boucher G, Brand S, Büning C, Cohain A, Cichon S, D'Amato M, De Jong D, Devaney KL, Dubinsky M, Edwards C, Ellinghaus D, Ferguson LR, Franchimont D, Fransen K, Gearry R, Georges M, Gieger C, Glas J, Haritunians T, Hart A, Hawkey C, Hedl M, Hu X, Karlsen TH, Kupcinskas L, Kugathasan S, Latiano A, Laukens D, Lawrance IC, Lees CW, Louis E, Mahy G, Mansfield J, Morgan AR, Mowat C, Newman W, Palmieri O, Ponsioen CY, Potocnik U, Prescott NJ, Regueiro M, Rotter JI, Russell RK, Sanderson JD, Sans M, Satsangi J, Schreiber S, Simms LA, Sventoraityte J, Targan SR, Taylor KD, Tremelling M, Verspaget HW, De Vos M, Wijmenga C, Wilson DC, Winkelmann J, Xavier RJ, Zeissig S, Zhang B, Zhang CK, Zhao H, International IBD Genetics Consortium (IIBDGC), Silverberg MS, Annese V, Hakonarson H, Brant SR, Radford-Smith G, Mathew CG, Rioux JD, Schadt EE, Daly MJ, Franke A, Parkes M, Vermeire S, Barrett JC, Cho JH. 2012. Host–microbe interactions have shaped the genetic architecture of inflammatory bowel disease. Nature 491:119–124. https://doi.org/10.1038/nature11582.
2. Parikh K, Antanaviciute A, Fawkner-Corbett D, Jagielowicz M, Aulicino A, Lagerholm C, Davis S, Kinchen J, Chen HH, Alham NK, Ashley N, Johnson E, Hublitz P, Bao L, Lukomska J, Andev RS, Björklund E, Kessler BM, Fischer R, Goldin R, Koohy H, Simmons A. 2019. Colonic epithelial cell diversity in health and inflammatory bowel disease. Nature 567:49–55. https://doi.org/10.1038/s41586-019-0992-y.
3. Graham DB, Xavier RJ. 2020. Pathway paradigms revealed from the genetics of inflammatory bowel disease. Nature 578:527–539. https://doi.org/10.1038/s41586-020-2025-2.
4. Chang JT. 2020. Pathophysiology of Inflammatory Bowel Diseases. N Engl J Med 383:2652–2664. https://doi.org/10.1056/NEJMra2002697.
5. Kostic AD, Xavier RJ, Gevers D. 2014. The microbiome in inflammatory bowel disease: current status and the future ahead. Gastroenterology 146:1489–1499. https://doi.org/10.1053/j.gastro.2014.02.009.
6. Rigottier-Gois L. 2013. Dysbiosis in inflammatory bowel diseases: the oxygen hypothesis. ISME J 7:1256–1261. https://doi.org/10.1038/ismej.2013.80.
7. Gevers D, Kugathasan S, Denson LA, Vázquez-Baeza Y, Treuren WV, Ren B, Schwager E, Knights D, Song SJ, Yassour M, Morgan XC, Kostic AD, Luo C, González A, McDonald D, Haberman Y, Walters T, Baker S, Rosh J, Stephens M, Heyman M, Markowitz J, Baldassano R, Griffiths A, Sylvester F, Mack D, Kim S, Crandall W, Hyams J, Huttenhower C, Knight R, Xavier RJ. 2014. The treatment-naïve microbiome in new-onset Crohn's disease. Cell Host Microbe 15:382–392. https://doi.org/10.1016/j.chom.2014.02.005.
8. Lupp C, Robertson ML, Wickham ME, Sekirov I, Champion OL, Gaynor EC, Finlay BB. 2007. Host-mediated inflammation disrupts the intestinal microbiota and promotes the overgrowth of Enterobacteriaceae. Cell Host Microbe 2:119–129. https://doi.org/10.1016/j.chom.2007.06.010.
9. Walters WA, Xu Z, Knight R. 2014. Meta-analyses of human gut microbes associated with obesity and IBD. FEBS Lett 588:4223–4233. https://doi.org/10.1016/j.febslet.2014.09.039.
10. Ni J, Wu GD, Albenberg L, Tomov VT. 2017. Gut microbiota and IBD: causation or correlation? Nat Rev Gastroenterol Hepatol 14:573–584. https://doi.org/10.1038/nrgastro.2017.88.
11. Tenaillon O, Skurnik D, Picard B, Denamur E. 2010. The population genetics of commensal *Escherichia coli*. Nat Rev Microbiol 8:207–217. https://doi.org/10.1038/nrmicro2298.
12. Kaper JB, Nataro JP, Mobley HLT. 2004. Pathogenic *Escherichia coli*. Nat Rev Microbiol 2:123–140. https://doi.org/10.1038/nrmicro818.
13. Leimbach A, Hacker J, Dobrindt U. 2013. *E. coli* as an all-rounder: the thin line between commensalism and pathogenicity, p 3–32. *In* Dobrindt U, Hacker JH, Svanborg C (ed), Between Pathogenicity and Commensalism. Springer, Berlin, Heidelberg.
14. Eaves-Pyles T, Allen CA, Taormina J, Swidsinski A, Tutt CBEE, Jezek G, Islas-Islas M, Torres AG. 2008. *Escherichia coli* isolated from a Crohn's disease patient adheres, invades, and induces inflammatory responses in polarized intestinal epithelial cells. Int J Med Microbiol 298:397–409. https://doi.org/10.1016/j.ijmm.2007.05.011.
15. Nash JH, Villegas A, Kropinski AM, Aguilar-Valenzuela R, Konczy P, Mascarenhas M, Ziebell K, Torres AG, Karmali MA, Coombes BK. 2010. Genome sequence of adherent-invasive *Escherichia coli* and comparative genomic analysis with other *E. coli* pathotypes. BMC Genomics 11:667. https://doi.org/10.1186/1471-2164-11-667.
16. Small C-LN, Reid-Yu SA, McPhee JB, Coombes BK. 2013. Persistent infection with Crohn's disease-associated adherent-invasive *Escherichia coli* leads to chronic inflammation and intestinal fibrosis. Nat Commun 4:1957. https://doi.org/10.1038/ncomms2957.
17. Darfeuille-Michaud A, Boudeau J, Bulois P, Neut C, Glasser A-L, Barnich N, Bringer M-A, Swidsinski A, Beaugerie L, Colombel J-F. 2004. High prevalence of adherent-invasive *Escherichia coli* associated with ileal mucosa in Crohn's disease. Gastroenterology 127:412–421. https://doi.org/10.1053/j.gastro.2004.04.061.
18. Glasser A-L, Boudeau J, Barnich N, Perruchot M-H, Colombel J-F, Darfeuille-Michaud A. 2001. Adherent invasive *Escherichia coli* strains from patients with Crohn's disease survive and replicate within macrophages without inducing host cell death. Infect Immun 69:5529–5537. https://doi.org/10.1128/IAI.69.9.5529-5537.2001.
19. Palmela C, Chevarin C, Xu Z, Torres J, Sevrin G, Hirten R, Barnich N, Ng SC, Colombel J-F. 2018. Adherent-invasive *Escherichia coli* in inflammatory bowel disease. Gut 67:574–587. https://doi.org/10.1136/gutjnl-2017-314903.
20. Shaler CR, Elhenawy W, Coombes BK. 2019. The unique lifestyle of Crohn's disease-associated adherent-invasive *Escherichia coli*. J Mol Biol 431:2970–2981. https://doi.org/10.1016/j.jmb.2019.04.023.
21. Dogan B, Suzuki H, Herlekar D, Sartor RB, Campbell BJ, Roberts CL, Stewart K, Scherl EJ, Araz Y, Bitar PP, Lefébure T, Chandler B, Schukken YH, Stanhope MJ, Simpson KW. 2014. Inflammation-associated adherent-invasive *Escherichia coli* are enriched in pathways for use of propanediol and iron and M-cell translocation. Inflamm Bowel Dis 20:1919–1932. https://doi.org/10.1097/MIB.0000000000000183.
22. Cieza RJ, Hu J, Ross BN, Sbrana E, Torres AG. 2015. The IbeA invasin of adherent-invasive *Escherichia coli* mediates interaction with intestinal epithelia and macrophages. Infect Immun 83:1904–1918. https://doi.org/10.1128/IAI.03003-14.

23. Sevrin G, Massier S, Chassaing B, Agus A, Delmas J, Denizot J, Billard E, Barnich N. 2020. Adaptation of adherent-invasive *E. coli* to gut environment: impact on flagellum expression and bacterial colonization ability. Gut Microbes 11:364–380. https://doi.org/10.1080/19490976.2017.1421886.
24. Viladomiu M, Metz ML, Lima SF, Jin W-B, Chou L, Guo C-J, Diehl GE, Simpson KW, Scherl EJ, Longman RS, JRI Live Cell Bank. 2021. Adherent-invasive *E. coli* metabolism of propanediol in Crohn's disease regulates phagocytes to drive intestinal inflammation. Cell Host Microbe 29: 607–619.e8. https://doi.org/10.1016/j.chom.2021.01.002.
25. Chervy M, Barnich N, Denizot J. 2020. Adherent-invasive *E. coli:* update on the lifestyle of a troublemaker in Crohn's disease. Int J Mol Sci 21:3734. https://doi.org/10.3390/ijms21103734.
26. Oberc AM, Fiebig-Comyn AA, Tsai CN, Elhenawy W, Coombes BK. 2019. Antibiotics potentiate adherent-invasive *E. coli* infection and expansion. Inflamm Bowel Dis 25:711–721. https://doi.org/10.1093/ibd/izy361.
27. Micoli F, Bagnoli F, Rappuoli R, Serruto D. 2021. The role of vaccines in combatting antimicrobial resistance. Nat Rev Microbiol 19:287–302. https://doi.org/10.1038/s41579-020-00506-3.
28. Mike LA, Smith SN, Sumner CA, Eaton KA, Mobley HLT. 2016. Siderophore vaccine conjugates protect against uropathogenic *Escherichia coli* urinary tract infection. Proc Natl Acad Sci U S A 113:13468–13473. https://doi.org/10.1073/pnas.1606324113.
29. Sassone-Corsi M, Chairatana P, Zheng T, Perez-Lopez A, Edwards RA, George MD, Nolan EM, Raffatellu M. 2016. Siderophore-based immunization strategy to inhibit growth of enteric pathogens. Proc Natl Acad Sci U S A 113:13462–13467. https://doi.org/10.1073/pnas.1606290113.
30. Miethke M, Marahiel MA. 2007. Siderophore-based iron acquisition and pathogen control. Microbiol Mol Biol Rev 71:413–451. https://doi.org/10.1128/MMBR.00012-07.
31. Deriu E, Liu JZ, Pezeshki M, Edwards RA, Ochoa RJ, Contreras H, Libby SJ, Fang FC, Raffatellu M. 2013. Probiotic bacteria reduce *Salmonella* Typhimurium intestinal colonization by competing for iron. Cell Host Microbe 14:26–37. https://doi.org/10.1016/j.chom.2013.06.007.
32. Bachman MA, Lenio S, Schmidt L, Oyler JE, Weiser JN. 2012. Interaction of lipocalin 2, transferrin, and siderophores determines the replicative niche of *Klebsiella pneumoniae* during pneumonia. mBio 3:e00224-11. https://doi.org/10.1128/mBio.00224-11.
33. Garcia EC, Brumbaugh AR, Mobley HLT. 2011. Redundancy and specificity of *Escherichia coli* iron acquisition systems during urinary tract infection. Infect Immun 79:1225–1235. https://doi.org/10.1128/IAI.01222-10.
34. Sarowska J, Futoma-Koloch B, Jama-Kmiecik A, Frej-Madrzak M, Ksiazczyk M, Bugla-Ploskonska G, Choroszy-Krol I. 2019. Virulence factors, prevalence and potential transmission of extraintestinal pathogenic *Escherichia coli* isolated from different sources: recent reports. Gut Pathog 11:10. https://doi.org/10.1186/s13099-019-0290-0.
35. Raymond KN, Dertz EA, Kim SS. 2003. Enterobactin: an archetype for microbial iron transport. Proc Natl Acad Sci U S A 100:3584–3588. https://doi.org/10.1073/pnas.0630018100.
36. Goetz DH, Holmes MA, Borregaard N, Bluhm ME, Raymond KN, Strong RK. 2002. The Neutrophil lipocalin NGAL is a bacteriostatic agent that interferes with siderophore-mediated iron acquisition. Mol Cell 10:1033–1043. https://doi.org/10.1016/s1097-2765(02)00708-6.
37. Flo TH, Smith KD, Sato S, Rodriguez DJ, Holmes MA, Strong RK, Akira S, Aderem A. 2004. Lipocalin 2 mediates an innate immune response to bacterial infection by sequestrating iron. Nature 432:917–921. https://doi.org/10.1038/nature03104.
38. Fischbach MA, Lin H, Zhou L, Yu Y, Abergel RJ, Liu DR, Raymond KN, Wanner BL, Strong RK, Walsh CT, Aderem A, Smith KD. 2006. The pathogen-associated *iroA* gene cluster mediates bacterial evasion of lipocalin 2. Proc Natl Acad Sci U S A 103:16502–16507. https://doi.org/10.1073/pnas.0604636103.
39. Subashchandrabose S, Hazen TH, Brumbaugh AR, Himpsl SD, Smith SN, Ernst RD, Rasko DA, Mobley HLT. 2014. Host-specific induction of *Escherichia coli* fitness genes during human urinary tract infection. Proc Natl Acad Sci U S A 111:18327–18332. https://doi.org/10.1073/pnas.1415959112.
40. Elhenawy W, Hordienko S, Gould S, Oberc AM, Tsai CN, Hubbard TP, Waldor MK, Coombes BK. 2021. High-throughput fitness screening and transcriptomics identify a role for a type IV secretion system in the pathogenesis of Crohn's disease-associated *Escherichia coli*. Nat Commun 12: 2032. https://doi.org/10.1038/s41467-021-22306-w.
41. Martinez-Medina M, Naves P, Blanco J, Aldeguer X, Blanco JE, Blanco M, Ponte C, Soriano F, Darfeuille-Michaud A, Garcia-Gil LJ. 2009. Biofilm formation as a novel phenotypic feature of adherent-invasive *Escherichia coli* (AIEC). BMC Microbiol 9:202. https://doi.org/10.1186/1471-2180-9-202.
42. Chassaing B, Darfeuille-Michaud A. 2013. The σE pathway is involved in biofilm formation by Crohn's disease-associated adherent-invasive *Escherichia coli*. J Bacteriol 195:76–84. https://doi.org/10.1128/JB.01079-12.
43. Moschen AR, Gerner RR, Wang J, Klepsch V, Adolph TE, Reider SJ, Hackl H, Pfister A, Schilling J, Moser PL, Kempster SL, Swidsinski A, Orth Höller D, Weiss G, Baines JF, Kaser A, Tilg H. 2016. Lipocalin 2 Protects from inflammation and tumorigenesis associated with gut microbiota alterations. Cell Host Microbe 19:455–469. https://doi.org/10.1016/j.chom.2016.03.007.
44. Zollner A, Schmiderer A, Reider SJ, Oberhuber G, Pfister A, Texler B, Watschinger C, Koch R, Effenberger M, Raine T, Tilg H, Moschen AR. 2021. Faecal biomarkers in inflammatory bowel diseases: calprotectin versus lipocalin-2-a comparative study. J Crohns Colitis 15:43–54. https://doi.org/10.1093/ecco-jcc/jjaa124.
45. Kühn R, Löhler J, Rennick D, Rajewsky K, Müller W. 1993. Interleukin-10-deficient mice develop chronic enterocolitis. Cell 75:263–274. https://doi.org/10.1016/0092-8674(93)80068-p.
46. Maharshak N, Packey CD, Ellermann M, Manick S, Siddle JP, Huh EY, Plevy S, Sartor RB, Carroll IM. 2013. Altered enteric microbiota ecology in interleukin 10-deficient mice during development and progression of intestinal inflammation. Gut Microbes 4:316–324. https://doi.org/10.4161/gmic.25486.
47. Zhu W, Winter MG, Byndloss MX, Spiga L, Duerkop BA, Hughes ER, Büttner L, de Lima Romão E, Behrendt CL, Lopez CA, Sifuentes-Dominguez L, Huff-Hardy K, Wilson RP, Gillis CC, Tükel Ç, Koh AY, Burstein E, Hooper LV, Bäumler AJ, Winter SE. 2018. Precision editing of the gut microbiota ameliorates colitis. Nature 553:208–211. https://doi.org/10.1038/nature25172.
48. Mörbe UM, Jørgensen PB, Fenton TM, von Burg N, Riis LB, Spencer J, Agace WW. 2021. Human gut-associated lymphoid tissues (GALT); diversity, structure, and function. Mucosal Immunol 14:793–802. https://doi.org/10.1038/s41385-021-00389-4.
49. Brandtzaeg P. 2009. Mucosal immunity: induction, dissemination, and effector functions. Scand J Immunol 70:505–515. https://doi.org/10.1111/j.1365-3083.2009.02319.x.
50. Boudeau J, Glasser A-L, Masseret E, Joly B, Darfeuille-Michaud A. 1999. Invasive ability of an *Escherichia coli* strain isolated from the ileal mucosa of a patient with Crohn's disease. Infect Immun 67:4499–4509. https://doi.org/10.1128/IAI.67.9.4499-4509.1999.
51. Mantis NJ, Rol N, Corthésy B. 2011. Secretory IgA's complex roles in immunity and mucosal homeostasis in the gut. Mucosal Immunol 4:603–611. https://doi.org/10.1038/mi.2011.41.
52. Dupont A, Heinbockel L, Brandenburg K, Hornef MW. 2014. Antimicrobial peptides and the enteric mucus layer act in concert to protect the intestinal mucosa. Gut Microbes 5:761–765. https://doi.org/10.4161/19490976.2014.972238.
53. Johansson MEV, Sjövall H, Hansson GC. 2013. The gastrointestinal mucus system in health and disease. Nat Rev Gastroenterol Hepatol 10:352–361. https://doi.org/10.1038/nrgastro.2013.35.
54. Swidsinski A, Sydora BC, Doerffel Y, Loening-Baucke V, Vaneechoutte M, Lupicki M, Scholze J, Lochs H, Dieleman LA. 2007. Viscosity gradient within the mucus layer determines the mucosal barrier function and the spatial organization of the intestinal microbiota. Inflamm Bowel Dis 13: 963–970. https://doi.org/10.1002/ibd.20163.
55. Eckmann L, Kagnoff MF. 2005. Intestinal mucosal responses to microbial infection. Springer Semin Immunopathol 27:181–196. https://doi.org/10.1007/s00281-005-0207-5.
56. McPhee JB, Small CL, Reid-Yu SA, Brannon JR, Le Moual H, Coombes BK. 2014. Host defense peptide resistance contributes to colonization and maximal intestinal pathology by Crohn's disease-associated adherent-invasive *Escherichia coli*. Infect Immun 82:3383–3393. https://doi.org/10.1128/IAI.01888-14.
57. Morgan XC, Tickle TL, Sokol H, Gevers D, Devaney KL, Ward DV, Reyes JA, Shah SA, LeLeiko N, Snapper SB, Bousvaros A, Korzenik J, Sands BE, Xavier RJ, Huttenhower C. 2012. Dysfunction of the intestinal microbiome in inflammatory bowel disease and treatment. Genome Biol 13:R79. https://doi.org/10.1186/gb-2012-13-9-r79.
58. Lo Presti A, Zorzi F, Del Chierico F, Altomare A, Cocca S, Avola A, De Biasio F, Russo A, Cella E, Reddel S, Calabrese E, Biancone L, Monteleone G, Cicala M, Angeletti S, Ciccozzi M, Putignani L, Guarino MPL. 2019. Fecal and mucosal microbiota profiling in irritable bowel syndrome and inflammatory bowel disease. Front Microbiol 10:1655. https://doi.org/10.3389/fmicb.2019.01655.
59. Zoetendal EG, von Wright A, Vilpponen-Salmela T, Ben-Amor K, Akkermans ADL, de Vos WM. 2002. Mucosa-associated bacteria in the human gastrointestinal tract are uniformly distributed along the colon and differ from the community recovered from feces. Appl Environ Microbiol 68:3401–3407. https://doi.org/10.1128/AEM.68.7.3401-3407.2002.

60. Leonardi I, Gao IH, Lin W-Y, Allen M, Li XV, Fiers WD, De Celie MB, Putzel GG, Yantiss RK, Johncilla M, Colak D, Iliev ID. 2022. Mucosal fungi promote gut barrier function and social behavior via type 17 immunity. Cell 185:831–846.e14. https://doi.org/10.1016/j.cell.2022.01.017.
61. Kane SV, Sandborn WJ, Rufo PA, Zholudev A, Boone J, Lyerly D, Camilleri M, Hanauer SB. 2003. Fecal lactoferrin is a sensitive and specific marker in identifying intestinal inflammation. Am J Gastroenterol 98:1309–1314. https://doi.org/10.1111/j.1572-0241.2003.07458.x.
62. Nelson AL, Ratner AJ, Barasch J, Weiser JN. 2007. Interleukin-8 secretion in response to aferric enterobactin is potentiated by siderocalin. Infect Immun 75:3160–3168. https://doi.org/10.1128/IAI.01719-06.
63. Saha P, Yeoh BS, Xiao X, Golonka RM, Abokor AA, Wenceslau CF, Shah YM, Joe B, Vijay-Kumar M. 2020. Enterobactin induces the chemokine, interleukin-8, from intestinal epithelia by chelating intracellular iron. Gut Microbes 12:1841548. https://doi.org/10.1080/19490976.2020.1841548.
64. Ellermann M, Gharaibeh RZ, Fulbright L, Dogan B, Moore LN, Broberg CA, Lopez LR, Rothemich AM, Herzog JW, Rogala A, Gordon IO, Rieder F, Brouwer CR, Simpson KW, Jobin C, Sartor RB, Arthur JC. 2019. Yersiniabactin-producing adherent/invasive *Escherichia coli* promotes inflammation-associated fibrosis in gnotobiotic Il10−/− Mice. Infect Immun 87:e00587-19. https://doi.org/10.1128/IAI.00587-19.
65. Saleh E, Moody MA, Walter EB. 2016. Effect of antipyretic analgesics on immune responses to vaccination. Hum Vaccin Immunother 12:2391–2402. https://doi.org/10.1080/21645515.2016.1183077.
66. Rousset F, Garcia E, Defrance T, Péronne C, Vezzio N, Hsu DH, Kastelein R, Moore KW, Banchereau J. 1992. Interleukin 10 is a potent growth and differentiation factor for activated human B lymphocytes. Proc Natl Acad Sci U S A 89:1890–1893. https://doi.org/10.1073/pnas.89.5.1890.
67. Uranga CC, Arroyo P, Duggan BM, Gerwick WH, Edlund A. 2020. Commensal oral *Rothia mucilaginosa* produces enterobactin, a metal-chelating siderophore. mSystems 5:e00161-20. https://doi.org/10.1128/mSystems.00161-20.
68. Zhu W, Winter MG, Spiga L, Hughes ER, Chanin R, Mulgaonkar A, Pennington J, Maas M, Behrendt CL, Kim J, Sun X, Beiting DP, Hooper LV, Winter SE. 2020. Xenosiderophore utilization promotes *Bacteroides thetaiotaomicron* resilience during colitis. Cell Host Microbe 27:376–388.e8. https://doi.org/10.1016/j.chom.2020.01.010.
69. Maier L, Goemans CV, Wirbel J, Kuhn M, Eberl C, Pruteanu M, Müller P, Garcia-Santamarina S, Cacace E, Zhang B, Gekeler C, Banerjee T, Anderson EE, Milanese A, Löber U, Forslund SK, Patil KR, Zimmermann M, Stecher B, Zeller G, Bork P, Typas A. 2021. Unravelling the collateral damage of antibiotics on gut bacteria. Nature 599:120–124. https://doi.org/10.1038/s41586-021-03986-2.
70. Chairatana P, Zheng T, Nolan EM. 2015. Targeting virulence: salmochelin modification tunes the antibacterial activity spectrum of β-lactams for pathogen-selective killing of *Escherichia coli*. Chem Sci 6:4458–4471. https://doi.org/10.1039/c5sc00962f.
71. Amann RI, Binder BJ, Olson RJ, Chisholm SW, Devereux R, Stahl DA. 1990. Combination of 16S rRNA-targeted oligonucleotide probes with flow cytometry for analyzing mixed microbial populations. Appl Environ Microbiol 56:1919–1925. https://doi.org/10.1128/aem.56.6.1919-1925.1990.
72. Frey A, Di Canzio J, Zurakowski D. 1998. A statistically defined endpoint titer determination method for immunoassays. J Immunol Methods 221:35–41. https://doi.org/10.1016/s0022-1759(98)00170-7.